# Analysis of Low Complexity Adaptive Step-size Orthogonal Gradient-based FEQ for OFDM Systems

**Suchada Sitjongsataporn**[1], Non-member

## ABSTRACT

We propose two low complexity adaptive step-size mechanisms based on the normalised orthogonal gradient algorithm for frequency-domain equalisation in orthogonal frequency division multiplexing (OFDM) systems. These algorithms are derived from employing a mixed-subcarrier exponentially weighted least squares criterion. Two low complexity adaptive step-size approaches are investigated by exploiting an estimate of autocorrelation between previous and present weight-estimated mixed-subcarrier errors. We compare our approaches with a previously fixed step-size normalised orthogonal gradient adaptive algorithm and other existing algorithm for implementation. Simulation results demonstrate that the proposed algorithms can achieve good performance for involving an OFDM receiver.

**Keywords**: Frequency-domain equalisation (FEQ), mixed-subcarrier criterion, adaptive algorithm, OFDM systems

## 1. INTRODUCTION

Orthogonal frequency division multiplexing (OFDM) is an efficient multicarrier modulation to fight against delay spread or frequency-selective fading of wireless and wireline channels. This approach has been adopted in standards for several high-speed wireless and wireline data applications, including digital audio and video broadcasting and local area networks [1], [2] . For broadband channels, the conventional time-domain equalisation is impractical, according to long channel impulse response in time domain. The approach for frequency domain equalisation (FEQ) is based on the discrete Fourier transform (DFT) and its inverse (IDFT) between the time and frequency domains. In order to avoid intersymbol interference (ISI) and intercarrier interference (ICI), the cyclic prefix (CP) is added between OFDM-symbols in the transmitter. An OFDM receiver transforms the received signal to frequency domain by applying a DFT. It performs a separate FEQ for each subcarrier.

In OFDM theory, there is no overlapping between subcarriers (or tone) due to orthogonality. In practice, the orthogonal structure is generally destroyed by frequency-selective fading channel, leading to information interfering from adjacent subcarriers as intercarrier interference (ICI). In case, information of a particular subcarrier usually smear into the adjacent subcarriers and leave some residual energy in them. This leads to the idea of a mixed-subcarrier (or mixed-tone) cost function as presented in [3]. The solution of a mixed-tone multitap frequency-domain equalisation, called per-tone equalisation, design criterion for discrete multitone (DMT) system has been proposed. The mixed-tone exponentially weighted least squares criterion can be shown to offer an improved signal to noise ratio (SNR) of the tone of interest by recovering adaptively the knowledge of residual interfering signal energy from adjacent tones as introduced in [3] .

In order to improve the convergence properties, the orthogonal gradient adaptive (OGA) algorithm has been presented by using the orthogonal projection in conjunction with the filtered gradient adaptive (FGA) algorithm in [4]. When the forgetting-factor is optimised sample by sample whereas a fixed forgetting-factor is used for FGA algorithm. A normalised version of the OGA (NOGA) algorithm that is introduced with the mixed-tone cost function and fixed step-size presented in [5] . With the purpose of the good tracking behaviour and recovering to a steady-state, it is necessary to let the step-size automatically track the change of system. A low complexity variable step-size mechanism has been presented from the idea of time averaging adaptive step-size criterion for adaptive beamforming in [6], [7] and for wireless systems in [8]. Consequently, the concept of low complexity adaptive step-size approach based on the FGA algorithm is introduced for the per-tone equalisation in DMT-based systems in [9].

In this paper, we propose two low complexity orthogonal gradient-based algorithms for FEQ in OFDM system based on the adaptive step-size (AS) algorithms related to the mixed-subcarrier criterion. Both low complexity modified adaptive step-size (MAS) and adaptive averaging step-size (AAS) algorithms have been developed for the FGA-based FEQ.

Manuscript received on August 12, 2011 ; revised on October 20, 2011.

[1] The author is with the Centre of Electronic Systems Design and Signal Processing (CESdSP) Department of Electronic Engineering, Mahanakorn University of Technology 140 Cheumsamphan Road, Nong-chok, Bangkok, 10530, Thailand., Email: ssuchada@mut.ac.th

The proposed algorithms can perform the tracking and convergence speed as compared with the fixed step-size algorithm.

The rest of the paper is structured as follows. We describe concisely the OFDM system model and notation in Section 2. The mixed-subcarrier criterion is presented in Section 3. With this criterion, the low complexity MAS and AAS mechanisms based on the NOGA-based algorithm are derived for updating the complex-valued FEQ framework in Section 4. Complexity and performance analysis of proposed algorithms are introduced in Section 5.and Section 6. Simulation results are shown in Section 7. Finally, Section 8. concludes the paper.

## 2. SYSTEM MODEL AND NOTATION

In this section, we explain briefly the baseband OFDM system model. At the transmitter, the input binary bit stream is fed into a serial-to-parallel converter. Then, each data stream modulates the corresponding subcarrier by quadrature phase shift keying (QPSK) or quadrature amplitude modulation (QAM). The modulated data symbols are then transformed by the inverse fast Fourier transform (IFFT).

The output symbols $x(k)$ are given by

$$x(k)=\frac{1}{\sqrt{\mathbb{M}}}\sum_{m=0}^{\mathbb{M}-1}\mathbf{X}(m)e^{j2\pi(km/\mathbb{M})},\quad 0\le k\le \mathbb{M}-1. \quad (1)$$

where $\mathbb{M}$ denotes as the number of subcarriers in the OFDM system. The cyclic prefix (CP) symbols are added in front of each frame of the IFFT output symbols in order to avoid ISI. After that, the parallel data are converted back to a serial data stream and transmitted over the frequency-selective channel with additive white Gaussian noise (AWGN).

The channel model can be described by

$$y(k)=\sum_{l=0}^{L-1}h_l x(k-l)+\eta(k)\ ,\quad 0\le k\le \mathbb{M}-1\ . \quad (2)$$

where $h_l$ denotes as the channel impulse response (CIR), which represents a frequency-selective Rayleigh fading channel. The parameter $L$ is the length of the CIR, where $0\le l\le L-1$. The i.i.d. complex-valued Gaussian random variables $\eta(k)$ is included with zero mean and variance $\sigma^2$ for both real and imaginary components, where $0\le k\le \mathbb{M}-1$.

The received data after removing the CP symbols are converted by applying FFT at the receiver. In the frequency domain, the received data are obtained by

$$\mathbf{Y}(m)=\frac{1}{\sqrt{\mathbb{M}}}\sum_{k=0}^{\mathbb{M}-1}y(k)e^{j2\pi(km/\mathbb{M})},\quad 0\le m\le \mathbb{M}-1. \quad (3)$$

where $\mathbb{M}$ is the number of subcarriers in the OFDM system.

Some notation will be used throughout this paper as follows: the operator $(\cdot)^H$ and $(\cdot)^*$ denote as the Hermitian and complex conjugate operators, respectively. A tilde over the variable indicates the frequency-domain. The vectors are in bold lowercase and matrices are in bold uppercase.

## 3. A MIXED-SUBCARRIER COST FUNCTION

In this section, we describe shortly how to define a mixed-subcarrier cost function by means of the orthogonal projection matrix. We refer the readers to [3] for more details.

The idea of using orthogonal projection of adjacent equalisers to include the information of interfering subcarriers has been presented in [3]. A mixed-subcarrier cost function derived as the sum of weight-estimated errors is optimised in order to achieve the solutions for frequency-domain equalisation (FEQ). It is designed to work in conjunction with the complex-valued FEQ structure.

A mixed-subcarrier exponentially weighted least squares cost function to be minimised is defined as

$$J(k)=\frac{1}{2}\sum_{m=1}^{M}\sum_{i=1}^{k}\lambda_m^{k-i}\{\xi_m(i)\}^{\,2}, \quad (4)$$

and

$$\xi_m(i)=\tilde{x}_m(i)-\hat{\mathbf{p}}_m^H(k)\tilde{\mathbf{y}}_m(i)-\sum_{l=1}^{L}\big(\Pi_l^{\perp}(k)\hat{\mathbf{p}}_l(k)\big)^H\tilde{\mathbf{y}}_l(i),\quad \text{for } m\ne l\ , L\le M-1 \quad (5)$$

where $\lambda_m$ is the forgetting-factor and $\xi_m(k)$ is the mixed-subcarrier weight-estimated error at subcarrier $m$ for $m\in M$. The number of the adjacent subcarriers $M$ is of subcarrier of interest. The parameter $\tilde{x}_m(k)$ is the $k^{th}$ transmitted OFDM-symbol on subcarrier $m$. The vector $\hat{\mathbf{p}}_m(k)$ is of complex-valued $\mathbb{T}$-tap FEQ for subcarrier $m$. The vector $\tilde{\mathbf{y}}_m(k)$ is the DFT output for subcarrier $m$ at symbol $k$. The orthogonal projection matrix $\Pi_l^{\perp}(k)$ of the tap-weight estimated vector $\hat{\mathbf{p}}_l(k)$ can be derived as [10]

$$\Pi_l^{\perp}(k)=\tilde{\mathbf{I}}-\hat{\mathbf{p}}_l(k)\,[\hat{\mathbf{p}}_l^H(k)\,\hat{\mathbf{p}}_l(k)]^{-1}\,\hat{\mathbf{p}}_l^H(k)\ , \quad (6)$$

where $\tilde{\mathbf{I}}$ denotes as an identity matrix. We note that the orthogonal projection matrix $\Pi_l^{\perp}(k)$ is mentioned by the vector $\hat{\mathbf{p}}_l(k)$ for $l\ne m$.

With the definition for this cost function, the $m^{th}$-term on the right hand side of (5) represents as the estimated mixed-subcarrier error of the symbol $k$ due to the $m^{th}$-subcarrier of equaliser $\hat{\mathbf{p}}_m(k)$ for $m\in M$.

## 4. LOW COMPLEXITY ADAPTIVE STEP-SIZE NORMALISED ORTHOGONAL GRADIENT ADAPTIVE ALGORITHMS

Based on filtered gradient adaptive algorithm, adaptive algorithms employing orthogonal gradient filtering can provide with the development of simple and robust filter across a wide range of input environments. This section is therefore concerned with the development of simple and robust adaptive frequency-domain equalisation by defining normalised orthogonal gradient adaptive algorithm.

In this section, we describe a class of the filtered gradient adaptive (FGA) algorithm in Section 4.1using an orthogonal constraint called the orthogonal gradient adaptive (OGA) algorithm. This employs the mixed-subcarrier criterion described above in Section 3in order to improve the convergence speed presented in Section 4.2respectively.

The idea for low complexity adaptive step-size algorithms with the mixed-subcarrier cost function is described in Section 4.3 For a large prediction error, the algorithm will increase the step-size to track the change of system whereas a small error will result in the decreased step-size [6].

### 4.1 A Filtered Gradient Adaptive (FGA) algorithm

This section reviews the derivation of the filtered gradient adaptive (FGA) algorithm by following [4]. The objective function is to obtain a recursive form as

$$\breve{J}(k) = \lambda_m(k)\ \breve{J}(k-1) + \frac{1}{2}\sum_{m=1}^{M}\{e_m(k)\}^{\ 2}\ , \quad (7)$$

$$e_m(k) = \tilde{x}_m(k) - \tilde{\mathbf{p}}_m^H(k)\tilde{\mathbf{y}}_m(k)\ , \quad (8)$$

where $\lambda_m(k)$ is the forgetting-factor and $e_m(k)$ is the weight-estimated error at symbol $k$ for $m \in M$.

The updating equation of the tap-weight estimated vector $\tilde{\mathbf{p}}_m(k)$ for each subcarrier $m$ at symbol $k$ can be expressed as

$$\tilde{\mathbf{p}}_m(k) = \tilde{\mathbf{p}}_m(k-1) + \mu\,\breve{\mathbf{d}}_m(k)\ , \quad (9)$$

where the updating process is performed along the direction vector $\breve{\mathbf{d}}_m(k)$ regulated by step-size $\mu$.

The direction vector $\breve{\mathbf{d}}_m(k)$ is chosen to be the negative gradient of the objective function in (7) as

$$\breve{\mathbf{d}}_m(k) \ = \ -\nabla_{\hat{\mathbf{p}}_m(k)}\breve{J}(k)\ . \quad (10)$$

Therefore, the update of direction vector $\breve{\mathbf{d}}_m(k)$ can be obtained in the recursion form as

$$\breve{\mathbf{d}}_m(k) \ = \ \lambda_m(k)\,\breve{\mathbf{d}}_m(k-1) + \breve{\mathbf{g}}_m(k)\ , \quad (11)$$

where $\breve{\mathbf{g}}_m(k)$ is the updated gradient vector which corresponds to filtering the instantaneous gradient as

$$\breve{\mathbf{g}}_m(k) = \tilde{\mathbf{y}}_m(k)\,e_m^*(k)\ , \quad (12)$$

and $e_m^*(k)$ is the complex conjugate of the estimated error as given in (8).

### 4.2 A Mixed-Subcarrier Normalised Orthogonal Gradient Adaptive (MS-NOGA) algorithm

The orthogonal gradient adaptive (OGA) algorithm is formulated from the FGA algorithm by introducing an orthogonal constraint between the present and previous direction vectors [11]. This OGA algorithm employs the optimised forgetting-factor on a sample-by-sample basis, so that the direction vector is orthogonal to the previous direction vector.

We then demonstrate the derivation of the mixed-subcarrier normalised orthogonal gradient adaptive (MS-NOGA) algorithm for FEQ in OFDM-based systems. With this mixed-subcarrier criterion in Section 3, the tap-weight estimate vector $\hat{\mathbf{p}}_m(k)$ at symbol $k$ for $m \in M$ can be obtained adaptively as

$$\hat{\mathbf{p}}_m(k) = \hat{\mathbf{p}}_m(k-1) + \mu_m(k)\,\mathbf{d}_m(k)\ , \quad (13)$$

where $\mu_m(k)$ is the step-size parameter and $\mathbf{d}_m(k)$ is the $\mathbb{T}\times 1$ direction vector.

The direction vector $\mathbf{d}_m(k)$ is given recursively as

$$\mathbf{d}_m(k) = \lambda_m(k)\,\mathbf{d}_m(k-1) + \mathbf{g}_m(k)\ , \quad (14)$$

where $\mathbf{g}_m(k)$ is the negative gradient of cost function $J(k)$ in (4) and $\lambda_m(k)$ is the forgetting-factor at symbol $k$.

By differentiating $J(k)$ in (4) with respect to $\hat{\mathbf{p}}_m(k)$, we then get the gradient vector $\mathbf{g}_m(k)$ as

$$\begin{aligned}\mathbf{g}_m(k) &= -\nabla_{\hat{\mathbf{p}}_m(k)}J(k)\\ &= -\xi_m(k)\,\frac{\partial\xi_m(k)}{\partial\hat{\mathbf{p}}_m(k)} = \tilde{\mathbf{y}}_m(k)\,\xi_m^*(k).\end{aligned} \quad (15)$$

where $\xi_m(k)$ is the mixed-subcarrier weight-estimated error at symbol $k$ for $m \in M$ as

$$\xi_m(k) \ = \ \tilde{x}_m(k) - \hat{\mathbf{p}}_m^H(k)\tilde{\mathbf{y}}_m(k) - \sum_{l=1}^{L}\left(\Pi_l^{\perp}(k)\hat{\mathbf{p}}_l(k)\right)^H\tilde{\mathbf{y}}_l(k). \quad \text{for } m\neq l\ ,\ L\leq M-1 \quad (16)$$

We introduce the updating gradient vector $\mathbf{g}_m(k)$ by

$$\mathbf{g}_m(k) = \lambda_m(k)\mathbf{g}_m(k-1) + \tilde{\mathbf{y}}_m(k)\xi_m^*(k)\ , \quad (17)$$

where $\xi_m^*(k)$ is the complex conjugate of the mixed-subcarrier estimated error at symbol $k$ for $m \in M$ as given in (16).

A procedure of an orthogonal gradient adaptive (OGA) algorithm to determine $\lambda_m(k)$ has been described in [11] by projecting the gradient vector $\mathbf{g}_m(k)$ onto the previous direction vector $\mathbf{d}_m(k-1)$. This leads us to obtain the direction vector $\mathbf{d}_m(k)$.

By determining the direction vector $\mathbf{d}_m(k)$ through an orthogonal projection of the gradient vector $\mathbf{g}_m(k)$ onto the previous direction vector $\mathbf{d}_m(k-1)$, we arrive

$$\mathbf{d}_m(k) = \mathbf{g}_m(k) - \frac{\mathbf{d}_m(k-1)\,\mathbf{d}_m^H(k-1)}{\mathbf{d}_m^H(k-1)\,\mathbf{d}_m(k-1)}\mathbf{g}_m(k)\ . \quad (18)$$

Thus, $\mathbf{d}_m(k)$ is orthogonal to the previous direction vector $\mathbf{d}_m(k-1)$ weighted by the forgetting-factor $\lambda_m(k)$. We can easily optimise a value of $\lambda_m(k)$ based on a sample-by-sample basis by taking the previous direction vector $\mathbf{d}_m(k-1)$ in (14) and setting to zero as

$$\mathbf{d}_m^H(k)\mathbf{d}_m(k-1) = \lambda_m(k)\mathbf{d}_m^H(k-1)\mathbf{d}_m(k-1) + \mathbf{g}_m^H(k)\mathbf{d}_m(k-1) = 0\ . \quad (19)$$

Meanwhile, the gradient vector $\mathbf{g}_m(k)$ becomes the direction vector $\mathbf{d}_m(k)$ when the gradient vector $\mathbf{g}_m(k)$ is orthogonal to previous direction vector $\mathbf{d}_m(k-1)$ by

$$\mathbf{g}_m^H(k)\mathbf{d}_m(k-1) = 0\ . \quad (20)$$

The forgetting-factor parameter $\lambda_m(k)$ can be calculated for each subcarrier $m$ at symbol $k$ as

$$\lambda_m(k) \quad = \quad \frac{\mathbf{g}_m^H(k)\,\mathbf{d}_m(k-1)}{\mathbf{d}_m^H(k-1)\,\mathbf{d}_m(k-1)}\quad . \quad (21)$$

According to the results in [4], it is noticed that the results of FGA and OGA algorithms are similar to those obtained by the normalised version of OGA (NOGA) algorithm. The convergence rate of the NOGA algorithm is shown that it is better than that of both FGA and OGA.

Therefore, we introduce the mixed-subcarrier normalised orthogonal gradient adaptive (MS-NOGA) algorithm which can be applied recursively as

$$\tilde{\mathbf{g}}_m(k) = \lambda_m(k)\tilde{\mathbf{g}}_m(k-1) + \frac{\tilde{\mathbf{y}}_m(k)\xi_m^*(k)}{\|\tilde{\mathbf{y}}_m(k)\|^2}\ , \quad (22)$$

where $\tilde{\mathbf{g}}_m(k)$ is obtained instead of the gradient vector $\mathbf{g}_m(k)$ in (17) and (21) for this normalised version.

In the state-space notation, the tap-weight estimated FEQ vector $\hat{\mathbf{p}}_m(k)$ for $m \in M$ can be performed using the proposed mixed-subcarrier normalised orthogonal gradient adaptive (MSNOGA) algorithm in (23)-(25), where $\mu_m(k)$ will be shown in Section 4.3 based on the proposed low complexity adaptive step-size algorithms.

### 4.3 Proposed Adaptive Step-size algorithms

This section describes the proposed low complexity adaptive step-size algorithms with the method of the mixed-subcarrier criterion as described in Section 3. as follows.

*1)Modified Adaptive Step-size algorithm (MAS)*: Following [12] and [13], the step-size parameter is controlled by squared prediction mixed-subcarrier error. If a large error will be the cause of increased step-size for fast tracking, while a small error will result in a decreased step-size to yield smaller misadjustment. This algorithm can be expressed as

$$\mu_m(k+1) = \gamma\,\mu_m(k) + \beta|\xi_m(k)|^2\ , \quad (26)$$

where $0 < \gamma < 1$, $\beta > 0$ and $\xi_m(k)$ is the mixed-subcarrier estimated error at symbol $k$ for $m \in M$ as given in (16).

We note that the step-size $\mu_m(k)$ is controlled by the instantaneous mixed-subcarrier cost function. The idea is that a large prediction errror causes the step-size to increase and provides faster tracking, while a small prediction error will result in a decrease in the step-size to yield smaller misadjustment.

The step-size parameter $\mu_m(k)$ at symbol $k$ for $m \in M$ is always positive and is controlled by the size of the prediction error and parameters $\alpha$ and $\beta$.

*2)Adaptive Averaging Step-size algorithm (AAS)*: The objective is to ensure large step-size $\mu_m(k)$ when the algorithm is far from an optimum point with $\mu_m(k)$ decreasing as we approach the optimum [6].

This algorithm achieves the objective using an estimate of the autocorrelation between $\xi_m(k)$ and $\xi_m(k-1)$ to control step-size update. The estimate of an averaging of $\xi_m(k)\cdot\xi_m(k-1)$ is introduced as

$$\mu_m(k+1) = \gamma\,\mu_m(k) + \beta\,|\hat{\zeta}_m(k)|^2\ , \quad (27)$$

$$\hat{\zeta}_m(k) = \alpha\,\hat{\zeta}_m(k-1) + (1-\alpha)\xi_m^*(k)\cdot\xi_m(k-1)\ , \quad (28)$$

where $0 < \gamma < 1$ and $\beta$ is an independent variable for scaling the prediction error. The exponentially weighting parameter $\alpha$ should be close to 1. The parameter $\xi_m^*(k)$ is the complex conjugate of the mixed-subcarrier estimated error at symbol $k$ for $m \in M$ as shown in (24).

The use of $\hat{\zeta}(k)$ responds to two objectives [6]. First, the error autocorrelation is generally a good measure for the optimum. Second, it rejects the effect of the uncorrelated noise sequence on the update step-size.

## 5. COMPUTATIONAL COMPLEXITY

In this section, we investigate the additional computational complexity of the proposed low complexity MAS and AAS algorithms. We consider that a multiplication of two complex numbers is counted as 4-real multiplications and 2-real additions. A multiplication of a real number with a complex number is computed by 2-real multiplications.

The proposed AAS mechanism involves two additional updates (27) and (28) as while the proposed

$$\begin{bmatrix} \hat{\mathbf{p}}_m(k) \\ \mathbf{d}_m(k) \\ \tilde{\mathbf{g}}_m(k) \end{bmatrix} = \begin{bmatrix} \mathbf{I} & \mu_m(k)\,\lambda_m(k)\mathbf{I} & \mu_m(k)\,\lambda_m(k)\,\mathbf{I} \\ \mathbf{0} & \lambda_m(k)\,\mathbf{I} & \lambda_m(k)\,\mathbf{I} \\ \mathbf{0} & \mathbf{0} & \lambda_m(k)\,\mathbf{I} \end{bmatrix} \cdot \begin{bmatrix} \hat{\mathbf{p}}_m(k-1) \\ \mathbf{d}_m(k-1) \\ \tilde{\mathbf{g}}_m(k-1) \end{bmatrix} + \begin{bmatrix} \frac{\mu_m(k)\,\tilde{\mathbf{y}}_m(k)\xi_m^*(k)}{\|\tilde{\mathbf{y}}_m(k)\|^2} \\ \frac{\tilde{\mathbf{y}}_m(k)\xi_m^*(k)}{\|\tilde{\mathbf{y}}_m(k)\|^2} \\ \frac{\tilde{\mathbf{y}}_m(k)\xi_m^*(k)}{\|\tilde{\mathbf{y}}_m(k)\|^2} \end{bmatrix} , \quad (23)$$

$$\text{where} \quad \xi_m(k) = \tilde{x}_m(k) - \hat{\mathbf{p}}_m^H(k-1)\tilde{\mathbf{y}}_m(k) - \sum_{l=1}^{L} \big(\Pi_l^{\perp}(k)\,\hat{\mathbf{p}}_l(k)\big)^H \tilde{\mathbf{y}}_l(k) \ , \quad \text{for} \quad m \neq l \ , \ L \leq M-1 \quad (24)$$

$$\lambda_m(k) = \frac{\tilde{\mathbf{g}}_m^H(k)\,\mathbf{d}_m(k-1)}{\|\mathbf{d}_m(k-1)\|^2} \ . \quad (25)$$

MAS approach employs only one update (26) compared with the fixed step-size (FS) MS-NOGA algorithm in [5].

Therefore, the computational complexity of the proposed MAS-MSNOGA, AAS-MSNOGA and FS-MSNOGA algorithms are listed in Table 1, where $\mathbb{T}$ is the number of taps of FEQ. It is shown that the proposed algorithms require a few fixed additional number of operations.

***Table 1:*** *The computational complexity per symbol.*

| Algorithm | Number of operations per symbol | | |
|---|---|---|---|
| | Multiplications | Additions | Divisions |
| MAS-MSNOGA | $8\mathbb{T}+5$ | $8\mathbb{T}+5$ | 1 |
| AAS-MSNOGA | $8\mathbb{T}+8$ | $8\mathbb{T}+6$ | 1 |
| FS-MSNOGA [5] | $8\mathbb{T}+2$ | $8\mathbb{T}+4$ | 1 |

## 6. PERFORMANCE ANALYSIS

The convergence behaviour and stability analysis of the proposed MAS and AAS mechanisms are investigated based on the mixed-subcarrier weight-estimated error. The convergence analysis of both MAS and AAS mechanisms are carried out the steady-state and mean-square expressions of the step-size parameter relating the mean convergence factor.

In the following analysis, we study the steady-state performance of the proposed MAS and AAS algorithms. We assume that these algortihms have converged.

### 6.1 Convergence analysis of the proposed MAS mechanism

Taking expectations on both sides of (26), the steady-state step-size arrives at

$$E\{\mu_m(k+1)\} = \gamma\, E\{\mu_m(k)\} + \beta\, E\{|\xi_m(k)|^2\} \ . \quad (29)$$

To facilitate the analysis, the proposed MAS mechanism is under a few assumptions.

***Assumption(i):*** We consider the steady-state value of $E\{\mu_m(k+1)\}$ by

$$\lim_{k\to\infty} E\{\mu_m(k+1)\} = \lim_{k\to\infty} E\{\mu_m(k)\} = E\{\mu_m(\infty)\} \ ,$$
$$\lim_{k\to\infty} E\{|\xi_m(k)|^2\} \ = \ \xi_m^{\min} + \xi_m^{\text{ex}}(\infty) \ ,$$

where $\xi_m^{\min}$ is the minimum mean square error (MMSE) and $\xi_m^{\text{ex}}(\infty)$ is the excess of mean square error (EMSE) related with the optimisation criterion in the steady-state condition.

Applying assumption (i) to (29), we obtain

$$E\{\mu_m(\infty)\} = \gamma\, E\{\mu_m(\infty)\} + \beta\, (\xi_m^{\min} + \xi_m^{\text{ex}}(\infty))$$
$$E\{\mu_m(\infty)\} = \frac{\beta\, (\xi_m^{\min} + \xi_m^{\text{ex}}(\infty))}{(1-\gamma)} \ . \quad (30)$$

To simplify these expressions, let us consider another assumption.

***Assumption(ii):*** Let us consider that for (30), where

$$\xi_m^{\min} + \xi_m^{\text{ex}}(\infty) \ \approx \ \xi_m^{\min} \ ,$$

and

$$\big(\xi_m^{\min} + \xi_m^{\text{ex}}(\infty)\big)^2 \ \approx \ \big(\xi_m^{\min}\big)^2 \ .$$

We then assume that $\xi_m^{\text{ex}}(\infty) \ll \xi_m^{\min}$, when the algorithm is close to optimum.

Employing assumption (ii) to (30), the steady-state step-size for the proposed MAS algorithm becomes

$$E\{\mu_m(\infty)\} \approx \frac{\beta\, (\xi_m^{\min})}{(1-\gamma)} \ . \quad (31)$$

It is noted that the steady-state performance of proposed MAS mechanism has derived in (31) for predicting in the steady-state condition.

### 6.2 Convergence analysis of the proposed AAS mechanism

Following [13] and [14], the average estimate $\hat{\zeta}_m(k)$ in (28) can be rewritten as

$$\hat{\zeta}_m(k) = (1-\alpha) \sum_{i=0}^{k-1} \alpha^i \xi_m^*(k-i)\xi_m(k-i-1) \ . \quad (32)$$

and

$$|\hat{\zeta}_m(k)|^2=(1-\alpha)^2\sum_{i=0}^{k-1}\sum_{j=0}^{k-1}\alpha^i\alpha^j\xi_m^*(k-i)\xi_m(k-i-1)\cdot \xi_m^*(k-j)\xi_m(k-j-1)\ . \tag{33}$$

We assume that the proposed algorithm has converged in the steady-state condition. Also, the expectation of (33) can be expressed as

$$E\{|\hat{\zeta}_m(k)|^2\}=(1-\alpha)^2\sum_{i=0}^{k-1}\alpha^{2i}\ E\{|\xi_m(k-i)|^2\}\cdot E\{|\xi_m(k-i-1)|^2\}\ , \tag{34}$$

where $\alpha$ is an exponential weighting parameter.

Using assumption (ii) into (34), we have

$$E\{|\hat{\zeta}_m(k)|^2\}=(1-\alpha)^2\ \mathcal{A}\ , \tag{35}$$

where

$$\mathcal{A}=(1+\alpha^2+\cdots+\alpha^{2k})(\xi_m^{\min}+\xi_m^{\mathrm{ex}}(\infty))^2\ . \tag{36}$$

By multiplying $\alpha^2$ on both sides of $\mathcal{A}$ in (36), if $k\to\infty$ and $0<\alpha<1$, we get

$$\begin{aligned}\alpha^2\ \mathcal{A}&=\alpha^2\cdot(1+\alpha^2+\ldots+\alpha^{2(k-1)}+\alpha^{2k})\cdot(\xi_m^{\min}+\xi_m^{\mathrm{ex}}(\infty))^2\\&=\mathcal{A}-(\xi_m^{\min}+\xi_m^{\mathrm{ex}}(\infty))^2\ .\end{aligned} \tag{37}$$

Rearranging (37) to get $\mathcal{A}$, we arrive at

$$\begin{aligned}(1-\alpha^2)\cdot\mathcal{A}&=(\xi_m^{\min}+\xi_m^{\mathrm{ex}}(\infty))^2\\ \mathcal{A}&=\frac{(\xi_m^{\min}+\xi_m^{\mathrm{ex}}(\infty))^2}{(1-\alpha^2)}\ .\end{aligned} \tag{38}$$

Substituting (38) into (35), we get

$$\begin{aligned}E\{|\hat{\zeta}_m(k)|^2\}&=\frac{(1-\alpha)^2\cdot(\xi_m^{\min}+\xi_m^{\mathrm{ex}}(\infty))^2}{(1-\alpha^2)}\\&=\frac{(1-\alpha)\cdot(\xi_m^{\min}+\xi_m^{\mathrm{ex}}(\infty))^2}{(1+\alpha)}\ .\end{aligned} \tag{39}$$

Taking the expectation on both sides of (27), the mean behaviour of step-size $\mu_m(k)$ is given as

$$E\{\mu_m(k+1)\}=\gamma E\{\mu_m(k)\}+\beta E\{|\hat{\zeta}_m(k)|^2\}\ . \tag{40}$$

Using assumption (i) and (39) into (40), we get

$$\begin{aligned}E\{\mu_m(\infty)\}&=\gamma E\{\mu_m(\infty)+\frac{\beta(1-\alpha)(\xi_m^{\min}+\xi_m^{\mathrm{ex}}(\infty))^2}{(1+\alpha)}\\E\{\mu_m(\infty)\}&=\frac{\beta(1-\alpha)(\xi_m^{\min}+\xi_m^{\mathrm{ex}}(\infty))^2}{(1-\gamma)(1+\alpha)}\ .\end{aligned} \tag{41}$$

where $\xi_m^{\min}$ is the steady-state minimum value and $\xi_m^{\mathrm{ex}}(\infty)$ is the steady-state excess error of mixed-subcarrier cost function.

By using assumption (ii), the steady-state value of $E\{\mu_m(\infty)\}$ in (41) is approximately as

$$E\{\mu_m(\infty)\}\approx\frac{\beta(1-\alpha)\left(\xi_m^{\min}\right)^2}{(1-\gamma)(1+\alpha)}\ . \tag{42}$$

We note that (42) has proven for predicting the steady-state performance of proposed AAS algorithm.

### 6.3 Stability and performance analysis

We introduce the stability and performance analysis of proposed algorithm that is based on the mean-squared value of the mixed-subcarrier estimated $\xi_m(k)$.

Let us denote the weight-error vector $\boldsymbol{\varepsilon}_m(k)$ at symbol $k$ for each subcarrier $m$ by [15] and [16]

$$\boldsymbol{\varepsilon}_m(k)=\mathbf{p}_{opt,m}-\hat{\mathbf{p}}_m(k)\ , \tag{43}$$

where $\mathbf{p}_{\mathrm{opt},m}$ denotes as the optimum Wiener solution for the tap-weight vector.

The estimate tap-weight FEQ vector $\hat{\mathbf{p}}_m(k)$ can be introduced as

$$\hat{\mathbf{p}}_m(k)=\hat{\mathbf{p}}_m(k-1)+\mu_m(k)\ \sum_{i=1}^{k}\lambda^{k-i}\frac{\tilde{\mathbf{y}}_m(i)\ \xi_m^*(i)}{\|\tilde{\mathbf{y}}_m^H(i)\ \tilde{\mathbf{y}}_m(i)\|}\ , \tag{44}$$

where $\xi_m(k)$ is the *a priori* mixed-subcarrier estimated error at symbol $k$ for subcarrier $m$ as

$$\xi_m(k)=\tilde{x}_m(k)-\hat{\mathbf{p}}_m^H(k-1)\tilde{\mathbf{y}}_m(k)-\sum_{l=1}^{L}(\Pi_l^{\perp}(k)\hat{\mathbf{p}}_l(k))^H\tilde{\mathbf{y}}_l(k)\ .\quad \text{for } m\neq l\ , L\leq M-1 \tag{45}$$

Subtracting $\mathbf{p}_{\mathrm{opt},m}$ from both sides of (44) and using (45) to eliminate $\hat{\mathbf{p}}_m(k)$, we may rewrite as shown in (46).

Substituting (43) in (46), we get

$$\begin{aligned}\boldsymbol{\varepsilon}_m(k)=\boldsymbol{\varepsilon}_m(k-1)&-\mu_m(k)\sum_{i=1}^{k}\lambda^{k-i}\frac{\tilde{\mathbf{y}}_m(i)\tilde{\mathbf{y}}_m^H(i)\boldsymbol{\varepsilon}_m(k-1)}{\|\tilde{\mathbf{y}}_m^H(i)\tilde{\mathbf{y}}_m(i)\|}\\&+\ \mu_m(k)\sum_{i=1}^{k}\lambda^{k-i}\frac{\tilde{\mathbf{y}}_m(i)}{\|\tilde{\mathbf{y}}_m^H(i)\tilde{\mathbf{y}}_m(i)\|}\Big\{\tilde{x}_m(i)-\mathbf{p}_{\mathrm{opt},m}^H\tilde{\mathbf{y}}_m(i)\\&-\sum_{l=1}^{L}(\Pi_l^{\perp}(i)\hat{\mathbf{p}}_l(k))^H\tilde{\mathbf{y}}_l(i)\Big\}^*\ .\end{aligned} \tag{47}$$

$$\big(\mathbf{p}_{opt,m}-\hat{\mathbf{p}}_m(k)\big)=\big(\mathbf{p}_{opt,m}-\hat{\mathbf{p}}_m(k-1)\big)+\mu_m(k)\sum_{i=1}^{k}\lambda^{k-i}\frac{\tilde{\mathbf{y}}_m(i)}{\|\tilde{\mathbf{y}}_m^H(i)\tilde{\mathbf{y}}_m(i)\|}\Big\{\tilde{x}_m(i)-\hat{\mathbf{p}}_m^H(k-1)\tilde{\mathbf{y}}_m(i)-\sum_{l=1}^{L}(\Pi_l^{\perp}(i)\hat{\mathbf{p}}_l(k))^H\tilde{\mathbf{y}}_l(i)\Big\}^*+\mu_m(k)\sum_{i=1}^{k}\lambda^{k-i}\frac{\tilde{\mathbf{y}}_m(i)}{\|\tilde{\mathbf{y}}_m^H(i)\tilde{\mathbf{y}}_m(i)\|}\big(\mathbf{p}_{opt,m}^H\tilde{\mathbf{y}}_m(i)\big)^*-\mu_m(k)\sum_{i=1}^{k}\lambda^{k-i}\frac{\tilde{\mathbf{y}}_m(i)}{\|\tilde{\mathbf{y}}_m^H(i)\tilde{\mathbf{y}}_m(i)\|}\big(\mathbf{p}_{opt,m}^H\tilde{\mathbf{y}}_m(i)\big)^* . \quad (46)$$

Then, the weight-error vector $\boldsymbol{\varepsilon}_m(k)$ can be expressed as

$$\boldsymbol{\varepsilon}_m(k)=\Big[\mathbf{I}-\mu_m(k)\sum_{i=1}^{k}\lambda^{k-i}\frac{\tilde{\mathbf{y}}_m(i)\tilde{\mathbf{y}}_m^H(i)}{\|\tilde{\mathbf{y}}_m^H(i)\tilde{\mathbf{y}}_m(i)\|}\Big]\boldsymbol{\varepsilon}_m(k-1)+\mu_m(k)\sum_{i=1}^{k}\lambda^{k-i}\frac{\tilde{\mathbf{y}}_m(i)}{\|\tilde{\mathbf{y}}_m^H(i)\tilde{\mathbf{y}}_m(i)\|}\,\xi_{\mathrm{opt},m}^* . \quad (48)$$

where $\xi_{\mathrm{opt},m}^*$ is the complex conjugate of estimation mixed-subcarrier error produced in the optimum Wiener solution as

$$\xi_{\mathrm{opt},m}=\tilde{x}_m(i)-\mathbf{p}_{\mathrm{opt},m}^H\tilde{\mathbf{y}}_m(i)-\sum_{l=1}^{L}(\Pi_l^{\perp}(i)\hat{\mathbf{p}}_l(k))^H\tilde{\mathbf{y}}_l(i). \quad \text{for } m\neq l\ , L\leq M-1 \quad (49)$$

***Assumption(iii):*** We consider the condition necessary for the convergence of mean, that is

$$E\{\,\|\boldsymbol{\varepsilon}_m(k)\|\,\}\to 0\ ,\quad \text{as}\quad k\to\infty$$

or equivalently,

$$E\{\,\hat{\mathbf{p}}_m(k)\,\}\to\mathbf{p}_{\mathrm{opt},m}\ ,\quad \text{as}\quad k\to\infty$$

where $\|\boldsymbol{\varepsilon}_m(k)\|$ is the Euclidean norm of the weight-error vector $\boldsymbol{\varepsilon}_m(k)$.

We denote the mixed-subcarrier estimated error for subcarrier $m$ at symbol $k$ as

$$\xi_m(k)=\tilde{x}_m(k)-\hat{\mathbf{p}}_m^H(k)\,\tilde{\mathbf{y}}_m(k)-\sum_{l=1}^{L}(\Pi_l^{\perp}(k)\hat{\mathbf{p}}_l(k))^H\tilde{\mathbf{y}}_l(k)\ . \quad \text{for } m\neq l\ , L\leq M-1 \quad (50)$$

Using (43) into (50), the estimation mixed-subcarrier error $\xi_m(k)$ at symbol $k$ for each subcarrier $m$ is given as in (51), where $\xi_{\mathrm{opt},m}$ is the estimation mixed-subcarrier error in the optimum Wiener solution shown in (49).

Let $J_m(k)$ denotes as the expectation of mean square error at subcarrier $m$ for $m\in M$

$$\begin{aligned}J_m(k)&=E\{\,|\xi_m(k)|^2\,\}\\&=E\{(\xi_{\mathrm{opt},m}+\boldsymbol{\varepsilon}_m^H(k)\tilde{\mathbf{y}}_m(k))^*(\xi_{\mathrm{opt},m}+\boldsymbol{\varepsilon}_m^H(k)\tilde{\mathbf{y}}_m(k))\}\\&=E\{|\xi_{\mathrm{opt},m}|^2\}+E\{\boldsymbol{\varepsilon}_m^H(k)\boldsymbol{\varepsilon}_m(k)\tilde{\mathbf{y}}_m^H(k)\tilde{\mathbf{y}}_m(k)\}\\&\quad+E\{\tilde{\mathbf{y}}_m^H(k)\boldsymbol{\varepsilon}_m(k)\xi_{\mathrm{opt},m}\}\\&\quad+E\{\boldsymbol{\varepsilon}_m^H(k)\tilde{\mathbf{y}}_m(k)\xi_{\mathrm{opt},m}^*\}\ .\end{aligned} \quad (52)$$

By using assumption (iii), we assume that

$$J_m(k)=J_m^{min}+J_m^{ex}(k)\ , \quad (53)$$

where $J_m^{min}$ is the minimum mean square error produced by the optimum Wiener filter for subcarrier $m$ as

$$J_m^{min}(k)=E\{|\xi_{\mathrm{opt},m}|^2\}+E\{\boldsymbol{\varepsilon}_m^H(k)\tilde{\mathbf{y}}_m(k)\xi_{\mathrm{opt},m}^*\}+E\{\tilde{\mathbf{y}}_m^H(k)\boldsymbol{\varepsilon}_m(k)\xi_{\mathrm{opt},m}\}\ , \quad (54)$$

and $J_m^{ex}(k)$ is called the excess mean square error (EMSE) at symbol $k$ for subcarrier $m$ as

$$J_m^{ex}(k)=E\{\,\boldsymbol{\varepsilon}_m^H(k)\boldsymbol{\varepsilon}_m(k)\tilde{\mathbf{y}}_m^H(k)\tilde{\mathbf{y}}_m(k)\,\}\ . \quad (55)$$

Since $\mathcal{R}_{\tilde{\mathbf{y}}\tilde{\mathbf{y}}}=E\{\tilde{\mathbf{y}}_m(k)\,\tilde{\mathbf{y}}_m^H(k)\}$ and by the orthogonality principle

$$E\{\xi_{\mathrm{opt},m}\,\tilde{\mathbf{y}}_m(k)\}\approx 0\ , \quad (56)$$

the excess in mean square error is given by

$$J_m^{ex}(k)=E\{\,\boldsymbol{\varepsilon}_m^H(k)\,\mathcal{R}_{\tilde{\mathbf{y}}\tilde{\mathbf{y}}}\,\boldsymbol{\varepsilon}_m(k)\,\}\ . \quad (57)$$

where $\boldsymbol{\varepsilon}_m(k)$ denotes as the weight-error vector at symbol $k$ for each subcarrier $m$ shown in (43).

## 7. SIMULATION RESULTS

In this section, we consider the performance of the proposed MAS-MSNOGA and AAS-MSNOGA algorithms compared with the fixed step-size approach introduced in [5] and the existing algorithm,

$$\xi_m(k) = \tilde{x}_m(k) - \hat{\mathbf{p}}_m^H(k)\,\tilde{\mathbf{y}}_m(k) - \sum_{l=1}^{L}(\Pi_l^{\perp}(k)\hat{\mathbf{p}}_l(k))^H\tilde{\mathbf{y}}_l(k)$$
$$= \tilde{x}_m(k) - (\mathbf{p}_{\mathrm{opt},m} - \boldsymbol{\varepsilon}_m(k))^H\tilde{\mathbf{y}}_m(k) - \sum_{l=1}^{L}(\Pi_l^{\perp}(k)\hat{\mathbf{p}}_l(k))^H\,\tilde{\mathbf{y}}_l(k)$$
$$= \tilde{x}_m(k) - \mathbf{p}_{\mathrm{opt},m}^H\,\tilde{\mathbf{y}}_m(k) - \sum_{l=1}^{L}(\Pi_l^{\perp}(k)\hat{\mathbf{p}}_l(k))^H\,\tilde{\mathbf{y}}_l(k) + \boldsymbol{\varepsilon}_m^H(k)\,\tilde{\mathbf{y}}_m(k) \;=\; \xi_{\mathrm{opt},m} + \boldsymbol{\varepsilon}_m^H(k)\,\tilde{\mathbf{y}}_m(k)\;. \quad (51)$$

namely the low complexity adaptive step-size algorithm presented in [7] in terms of bit error rate performance. The fixed step-size mechanism using the mixed-subcarrier criterion based on normalised orthogonal gradient adaptive (FS-MSNOGA) algorithm [5] is applied for frequency-domain equalisation (FEQ). An adaptive step-size (AS) mechanism [7] has been presented with the mean square error (MSE) criterion. This leads to apply for frequency-domain equalisation (FEQ) based on normalised orthogonal gradient adaptive (AS-NOGA) algorithm in the experiments.

In all simulations, firstly, the mean square error (MSE) performance is compared to evaluate the mechanisms in additive white Gaussian noise (AWGN) single-path channel. For the multipath channel, we then estimate a corrupted channel following the ITU-Pedestrian A [17] with AWGN. The bit error rate (BER) performance is taken into account, and at last we focus on the tracking and convergence speed of proposed algorithms.

We simulated an OFDM systems with the 16-QAM modulation, which is similar to the 802.11a specification in order to demonstrate the effectiveness of the proposed MAS-MSNOGA and AAS-MSNOGA algorithms based on the frequency-domain equalisation (FEQ), including with two experiments as the AWGN single-path channel and multipath corrupted AWGN channel. The entire channel bandwidth is of 20MHz and is divided into 64 subcarriers. The symbol duration is chosen as 3.2 $\mu$s. The total OFDM frame length is $T_s = 100\mu$s. The receiver processing consists of minimum mean square error (MMSE) frequency-domain equalisation, hard symbol decision and decoding. The fading gains are randomly generated by complex Gaussian distributed random variables with zero mean and unit variance.

The initial parameters of proposed MAS-MSNOGA, AAS-MSNOGA and FS-MSNOGA [5] FEQs are as follows: $\mathbb{T} = $ , $\hat{\mathbf{p}}_m(0) = \mathbf{d}_m(0) = \tilde{\mathbf{g}}_m(0) = [1\ 0\cdots 0]^T$, $\lambda_m(0) = 0.975$, $\Pi_m^{\perp}(k) = \mathbf{I}$, where $\mathbf{I}$ is an identity matrix. The use of 3-combining of adjacent subcarriers ($M = 3$) is employed for the estimate tap-weight FEQ vector $\hat{\mathbf{p}}_m(k)$ on subcarrier $m$. The other parameters of both proposed MAS-MSNOGA and AAS-MSNOGA algorithms have been optimised with $\gamma = 0.975$, $\alpha = 0.97$ and $\beta = 1.95 \times 10^{-3}$. The optimised parameters are chosen based on simulation results in order to achieve the good performance.

For the AS-NOGA [7] FEQs, the initial parameters are set to the same values as those of the proposed algorithms for FEQs except using the estimation error given in (8) for each subcarrier $m$ separately due to optimisation.

The first experiment investigated the performance of proposed MAS-MSNOGA and AAS-MSNOGA algorithms compared with the FS-MSNOGA [5] algorithm and adaptive step-size (AS) mechanism [7] with the mean square error criterion based on normalised orthogonal gradient adaptive (AS-NOGA) algorithm for AWGN channel. The subcarrirer $m = 30$ was a representative of simulations.

Fig. 1 and Fig. 2 illustrate the trajectories of adaptive step-size parameters $\mu_m(k)$ on subcarrier $m$ of proposed MAS-MSNOGA and AAS-MSNOGA FEQs at four different values of initial step-size settings of $\mu(0) = 9.5 \times 10^{-4}, 9.5 \times 10^{-3}, 3.95 \times 10^{-2}$ and $9.5 \times 10^{-2}$, respectively. Both of them are shown to converge to each equilibrium despite large variations in initial settings of step-size parameters with the samples of subcarriers, when SNR is of 20 dB.

Fig. 3 depicts the MSE performance of proposed MAS-MSNOGA and AAS-MSNOGA algorithms on subcarrier $m$ with using $\mu(0) = 9.5 \times 10^{-4}$ compared to the FS-MSNOGA [5] algorithm using the fixed step-size parameter at $\mu = 1.595 \times 10^{-4}$ and AS-NOGA [7] algorithm using $\mu(0) = 9.5 \times 10^{-4}$ for AWGN channel, where the signal to noise ratio (SNR) is of 20dB as a representative and $m = 30$. The proposed MAS-MSNOGA and AAS-MSNOGA algorithms can converge rapidly to steady-state condition with the low initial step-size parameter. It is noted that the proposed algorithms can acheive the same mean square error (MSE) performance as the FS-MSNOGA [5] and AS-NOGA [7] algorithms.

Fig. 4 indicates the BER performance of proposed MAS-MSNOGA and AAS-MSNOGA FEQs on subcarrier $m$ with using the same value of initial step-size $\mu(0) = 9.5 \times 10^{-4}$ as compared with the

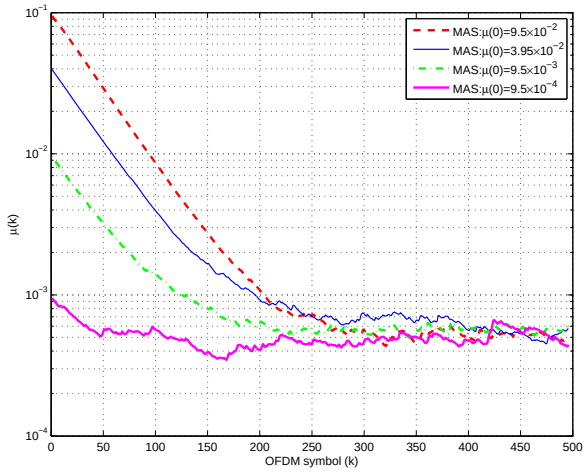


***Fig.1:*** *Trajectories of the adaptive step-size $\mu_m(k)$ of proposed MAS-MSNOGA algorithm with the samples of AWGN channel of subcarrier at $m = 30$ as a representativeusing different setting of $\mu(0)$, when SNR = 20dB.*

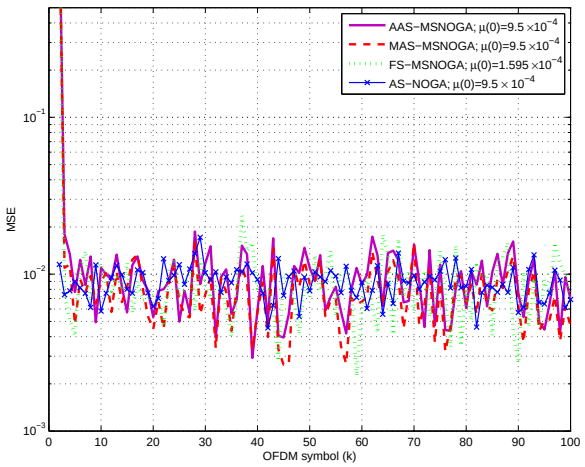


***Fig.3:*** *Learning curves of mean square error (MSE) of the proposed MAS and AAS mechanisms $\mu_m(k)$ compared with FS mechanism of MS-NOGA [5] algorithm and AS [7] mechanism of NOGA algorithm with the samples of AWGN channel of subcarrier at $m = 30$, when SNR=20dB.*

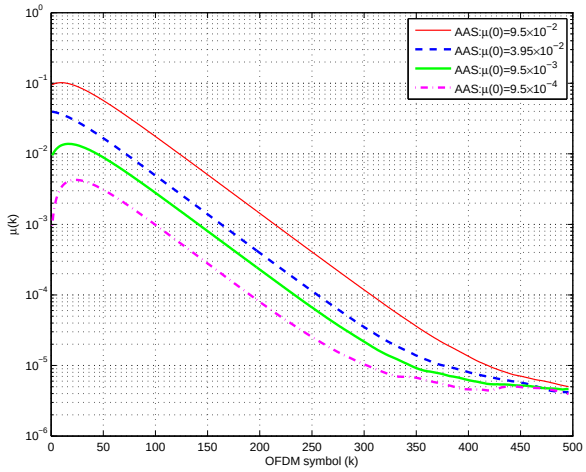


***Fig.2:*** *Trajectories of the adaptive step-size $\mu_m(k)$ of proposed AAS-MSNOGA algorithm with the samples of AWGN channel of subcarrier at $m = 30$ as a representative using different setting of $\mu(0)$, when SNR = 20dB.*

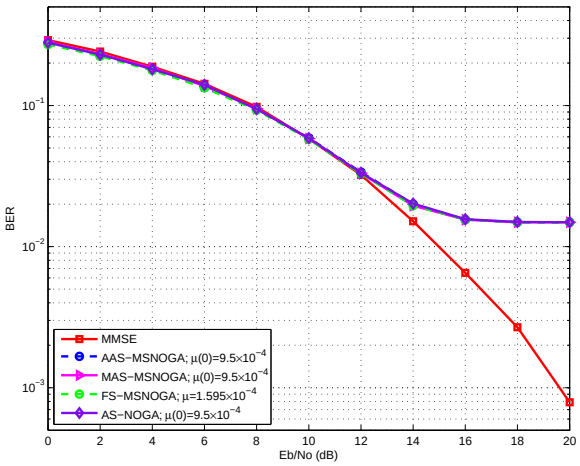


***Fig.4:*** *Bit error rate (BER) performance of OFDM-based systems with different types of proposed MAS-MSNOGA and AAS-MSNOGA FEQs in comparison with MMSE, FS-MSNOGA [5] and AS-NOGA [7] FEQs for AWGN channel.*

method of minimum mean square error (MMSE), FS-MSNOGA [5] FEQs using the fixed step-size $\mu = 1.595 \times 10^{-4}$ and AS-NOGA [7] FEQs using $\mu(0) = 9.5 \times 10^{-4}$ for AWGN channel, when SNR is of 20 dB and $m = 30$. It is noted that the BER of proposed MAS-MSNOGA and AAS-MSNOGA algorithms can achieve performance the same as those of the FS-MSNOGA [5] and AS-NOGA [7] algorithms. The BER performance of all FEQs based on NOGA algorithm can obtain the good performance close to the MMSE FEQs, when $E_b/N_0 \leq 15$dB.

The second experiment considered the performance of proposed MAS-MSNOGA and AAS-MSNOGA algorithms in comparison with the FS-MSNOGA [5] and AS-NOGA [7] algorithms in multipath channel [17] corrupted with AWGN, when $m = 30$ as a representative of simulations.

In Fig. 5 and Fig. 6, their results illustrate the adaptive step-size parameters $\mu_m(k)$ on subcarrier $m$ of proposed MAS-MSNOGA and AAS-MSNOGA FEQs at the same different values of initial step-size parameters as $\mu(0) = 9.5 \times 10^{-4}, 9.5 \times 10^{-3}, 3.95 \times$

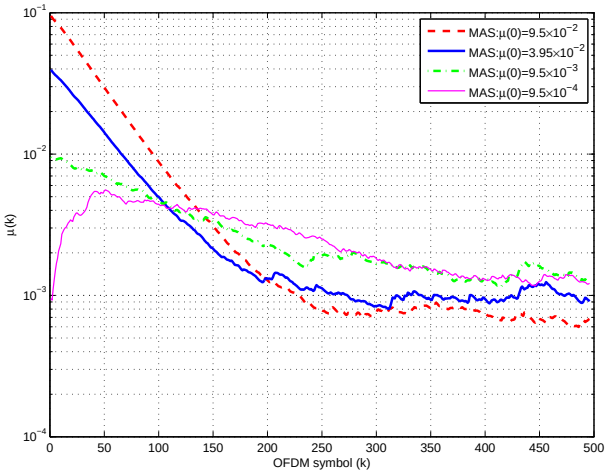


***Fig.5:*** *Trajectories of the adaptive step-size $\mu_m(k)$ of proposed MAS-MSNOGA algorithm with the samples of multipath channel of subcarrier at $m = 30$ as a representative using different setting of $\mu(0)$, when SNR = 20dB.*

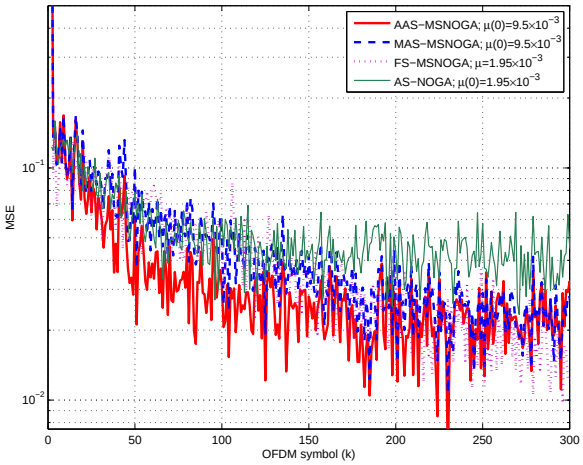


***Fig.7:*** *Learning curves of mean square error (MSE) of the proposed MAS and AAS mechanisms $\mu_m(k)$ compared with FS mechanism of MS-NOGA [5] algorithm and AS [7] mechanism of NOGA algorithm with the samples of multipath channel of subcarrier at $m = 30$, when SNR=20dB.*

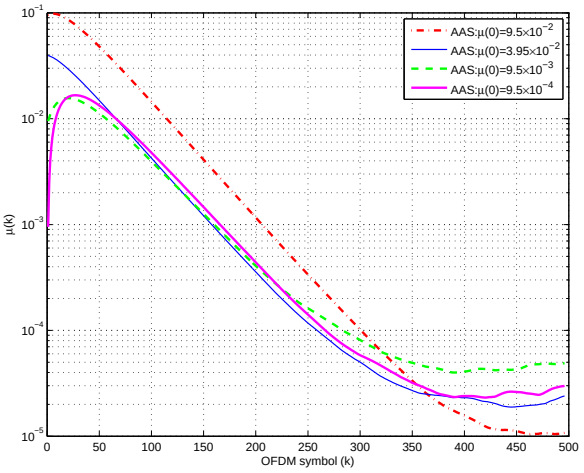


***Fig.6:*** *Trajectories of the adaptive step-size $\mu_m(k)$ of proposed AAS-MSNOGA algorithm with the samples of multipath channel of subcarrier at $m = 30$ as a representative using different setting of $\mu(0)$, when SNR = 20dB.*

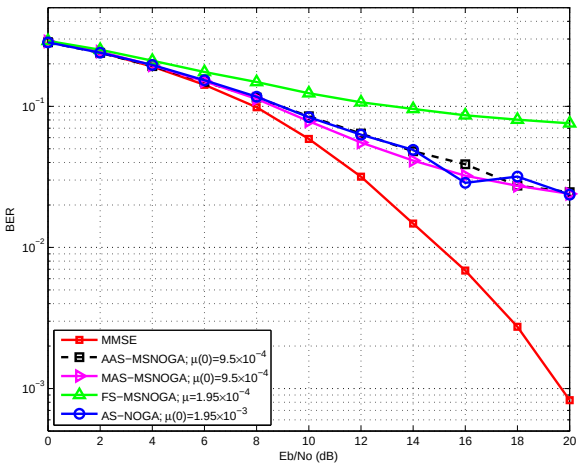


***Fig.8:*** *Bit error rate (BER) performance of OFDM-based systems with different types of proposed MAS-MSNOGA and AAS-MSNOGA FEQs in comparison with MMSE, FS-MSNOGA [5] and AS-NOGA [7] FEQs for multipath channel.*

$10^{-2}$ and $9.5 \times 10^{-2}$, where SNR is of 20dB and $m = 30$. They are shown clearly to converge to each equilibrium despite large variations in initial setting of step-size parameters with the corrupted AWGN and multipath channel in the OFDM-based system.

Fig. 7 shows the MSE performance of proposed MAS-MSNOGA and AAS-MSNOGA algorithms on subcarrier $m$ with the same value of initial step-size $\mu(0) = 9.5 \times 10^{-3}$ as compared to the FS-MSNOGA [5] algorithm using the fixed step-size parameter at $\mu = 1.95 \times 10^{-3}$ and AS-NOGA [7] algorithm using $\mu(0) = 1.95 \times 10^{-3}$, where SNR is of 20dB and $m = 30$. In this condition, the convergence of proposed AAS-MSNOGA algorithm outperforms the convergence of proposed MAS-MSNOGA, FS-MSNOGA [5] and AS-NOGA [7] algorithms in the multipath system with the same range of initial step-size parameters for AWGN single-path channel.

Fig. 8 indicates the BER performance of proposed MAS-MSNOGA and AAS-MSNOGA FEQs using the same value of initial step-size $\mu(0) = 9.5 \times 10^{-4}$ in comparison with the MMSE FEQs, FS-MSNOGA [5]

FEQs with the fixed step-size $\mu = 1.95 \times 10^{-4}$ and AS-NOGA [7] FEQs using $\mu(0) = 1.95 \times 10^{-3}$ for the multipath channel [17] corrupted with AWGN, when SNR is of 20 dB and $m = 30$. It is seen that the good performance can obtain with the proposed MAS-MSNOGA followed by the proposed AAS-MSNOGA, AS-NOGA [7] and FS-MSNOGA [5] algorithms, respectively. Both of BER performance of proposed MAS-MSNOGA and AAS-MSNOGA algorithms are still able to enhance performance close to the MMSE FEQs, when $E_b/N_0 \leq 10$dB for the multipath channel and corrupted with AWGN in the OFDM-based systems.

## 8. CONCLUSION

In this paper, we have proposed adaptive step-size mechanisms for frequency-domain equalisers (FEQs) based on the normalised orthogonal gradient-based algorithms in OFDM-based systems. We have described how to investigate the proposed MASS-MSNOGA and AAS-MSNOGA FEQs based on a solution of the mixed-subcarrier (MS) cost function. Two of low complexity adaptive step-size algorithms have been developed and analysed for the normalised version of orthogonal gradient adaptive algorithm based on this mixed-subcarrier criterion.

The performance of convergence and stability analysis have been investigated in terms of the excess mean square error. Both of the trajectories of adaptive step-size of proposed MAS-MSNOGA and AAS-MSNOGA algorithms are also shown to converge to each equilibrium despite 100-fold initial variations in both single-path and multipath channels. The MSE performance of proposed algorithms are shown to converge rapidly to steady-state condition. Our results indicate that the BER performance is acceptable in comparison with the fixed step-size algorithm and the several existing algorithms.

## References


[1] Y.Lin, S.Phoong and P.P.Vaidyanathan, *Filter Bank Tranceivers for OFDM and DMT systems*, Cambridge University Press, 2011.

[2] H.Schulze and C.Lüders, *Theory and Applications of OFDM and CDMA: Wideband Wireless Communications*, John Wiley, 2005.

[3] S.Sitjongsataporn and P.Yuvapoositanon, "A Mixed-Tone RLS Algorithm with Orthogonal Projection for Per-Tone DMT Equalisation", in *Proc. IEEE Midwest Symposium on Circuits and Systems (MWSCAS)*, Knoxville, USA, pp. 942-945, Aug. 2008.

[4] J.A.Apolinário Jr., R.G.Alves, P.S.R.Diniz and M.N.Swamy, "Filtered Gradient Algorithm Applied to a Subband Adaptive Filter Structure", in *Proc. IEEE International Conference Acoustics, Speech, and Signal Processing (ICASSP)*, vol.6, pp. 3705-3708, May 2001.

[5] S.Sitjongsataporn and P.Yuvapoositanon, "Mixed-Tone Normalised Orthogonal Gradient Adaptive Per-Tone DMT Equalisation", in *Proc. IEEE International Conference on Electrical Engineering/Electronics, Computer, Telecommunications and Information Technology (ECTI-CON)*, Pattaya, Thailand, pp. 1151-1154, May 2009.

[6] L.Wang, Y.Cai and R.C.de Lamare, "Low-Complexity Adaptive Step-Size Constrained Constant Modulus SG-based Algorithms for Blind Adaptive Beamforming", in *Proc. IEEE International Conference Acoustics, Speech, and Signal Processing (ICASSP)*, pp. 2593-2596, 2008.

[7] L.Wang, R.C.de Lamare and Y.Cai, "Low-Complexity Adaptive Step-Size Constrained Constant Modulus SG Algorithms for Adaptive Beamforming", *Signal Processing*, vol.89, pp. 2503-2513, 2009.

[8] R.C.de Lamare and R.Sampaio-Neto, "Low-Complexity Variable Step-Size Mechanisms for Stochastic Gradient Algorithms in Mimimum Variance CDMA Receivers", *IEEE Transactions on Signal Processing*, vol. 54, pp. 2302-2317, Jun. 2006.

[9] S.Sitjongsataporn and P.Yuvapoositanon, "Low Complexity Adaptive Step-size Filtered Gradient-based Per-Tone DMT Equalisation", in *Proc. IEEE International Symposium on Circuits and Systems (ISCAS)*, Paris, France, pp. 2526-2529, May 2010.

[10] G.Strang, *Linear Algebra and Its Applications*, Harcourt Brace Jovanovich, 1988.

[11] J.S.Lim, "New Adaptive Filtering Algorithm Based on an Orthogonal Projection of Gradient Vectors", *IEEE Signal Processing Letters*, vol. 7, no. 11, pp. 314-316, Nov. 2000.

[12] Y.Cai and R.C.de Lamare, "Low-complexity Variable Step-Size Mechanism for Code-Constrained Constant Modulus Stochastic Gradient Algorithms Applied to CDMA Interference Suppression", *IEEE Transactions on Signal Processing*, vol. 57, no. 1, pp. 313-323, Jan. 2009.

[13] R.H.Kwong and E.W.Johnston, "A Variable Step Size LMS Algorithm", *IEEE Transactions on Signal Processing*, vol.40, no.7, pp. 1633-1642, July 1992.

[14] T.Aboulnasr, and K.Mayyas, "A Robust Variable Step-Size LMS-Type Algorithm: Analysis and Simulations", *IEEE Transactions on Signal Processing*, vol. 45, no. 3, pp. 631-639, Mar. 1997.

[15] P.S.R.Diniz, *Adaptive Filtering: Algorithms and Practical Implementation*, Springer, 2008.

[16] S.Haykin, *Adaptive Filter Theory*, Prentice Hall,

1996.

[17] 3rd Generation Partnership Project, 3GPP TS 25.101 - *Technical Specification Group Radio Access Network; User Equipment (UE) Radio Transmission and Reception (FDD) (Release 9)*, June 2010.

**Suchada Sitjongsataporn** received the B.Eng. and D.Eng. degrees of Electrical Engineering from Mahanakorn University of Technology, Bangkok, Thailand in 2002 and 2009, respectively. She has worked as lecturer at department of Electronic Engineering, Mahanakorn University of Technology, since 2002. Her research interests are in the area of adaptive algorithm, adaptive equalisation and adaptive signal processing for wireline and wireless communications.